environmental microbiology

Environmental Microbiology (2022) **24**(9), 4124–4136 doi:10.1111/1462-2920.16036

Variations of microbial communities and substrate regimes in the eastern Fram Strait between summer and fall

Anabel von Jackowski,[1*] **Kevin W. Becker**,[1] **Matthias Wietz**,[2,3] **Christina Bienhold**,[2,3] **Birthe Zäncker**,[4] **Eva-Maria Nöthig**[2] **and Anja Engel**[1]

[1]*GEOMAR Helmholtz Centre for Ocean Research Kiel, Kiel, Germany.*

[2]*Alfred Wegener Institute Helmholtz Centre for Polar and Marine Research, Bremerhaven, Germany.*

[3]*Max Planck Institute for Marine Microbiology, Bremen, Germany.*

[4]*Marine Biological Association of the UK, The Laboratory, Citadel Hill, Plymouth, UK.*

Summary

Seasonal variations in day length and temperature, in combination with dynamic factors such as advection from the North Atlantic, influence primary production and the microbial loop in the Fram Strait. Here, we investigated the seasonal variability of biopolymers, microbial abundance and microbial composition within the upper 100 m during summer and fall. Flow cytometry revealed a shift in the autotrophic community from picoeukaryotes dominating in summer to a 34-fold increase of *Synechococcus* by fall. Furthermore, a significant decline in biopolymers concentrations covaried with increasing microbial diversity based on 16S rRNA gene sequencing along with a community shift towards fewer polymer-degrading genera in fall. The seasonal succession in the biopolymer pool and microbes indicates distinct metabolic regimes, with a higher relative abundance of polysaccharide-degrading genera in summer and a higher relative abundance of common taxa in fall. The parallel analysis of DOM and microbial diversity provides an important baseline for microbe–substrate relationships over the seasonal cycle in the Arctic Ocean.

Received 3 August, 2021; revised 22 April, 2022; accepted 3 May, 2022. *For correspondence. E-mail ajackowski@geomar.de. Tel. +49 431 600 4285.

Introduction

Marine phytoplankton release species-specific organic matter composed of high carbon and nitrogen, which is remineralized by heterotrophic microbes (Biersmith and Benner, 1998; Hedges *et al*., 2002). Organic matter is constantly produced and degraded, allowing it to be classified into either particulate organic matter (>0.7 μm) or dissolved organic matter (DOM; <0.7 μm) (Benner *et al*., 1992). Particularly DOM, as the largest carbon reservoir, can further be partitioned into the low-molecular-weight (<1 kDa) or high-molecular-weight fraction (>1 kDa) respectively (Hansell *et al*., 2009). The variable reactivity of low-molecular-weight DOM includes monomers such as free carbohydrates and amino acids, whereas high-molecular-weight DOM includes biopolymers such as dissolved combined carbohydrates (DCCHO) and dissolved hydrolyzable amino acids (DHAA).

DCCHO and DHAA serve as substrates for bacteria and archaea. For instance, *Flavobacteriaceae* are specialized in polysaccharide degradation suggesting a possible link to their prevalence during phytoplankton blooms in temperate and polar habitats (Kirchman *et al*., 2010; Wilson *et al*., 2017; Fadeev *et al*., 2018; Cardozo Mino *et al*., 2021). *Gammaproteobacteria* such as *Porticoccaceae* can be abundant in response to algal decay, as the release of high-molecular-weight DOM is particularly prominent during and towards the end of a phytoplankton bloom (Engel *et al*., 2011; Teeling *et al*., 2012).

In the Arctic Ocean, phytoplankton and microbes are controlled by pre-existing environmental conditions and are increasingly influenced by sea ice loss, glacial runoff, or permafrost melt (Boetius *et al*., 2015). For example, the seasonal cycles in light and nutrient availability are closely coupled to phytoplankton biomass in the Fram Strait (Randelhoff *et al*., 2018). As the productive season progresses, phytoplankton release biopolymers that promote the growth of microbial communities, which remineralize this organic matter (Piontek *et al*., 2014; von Jackowski *et al*., 2020). To continue understanding the substrate requirements of microbes, this study expands on demonstrated seasonal changes in biopolymer concentrations and microbial composition in the Fram Strait

as the primary inflow to the Arctic Ocean (von Jackowski *et al*., 2020; Wietz *et al*., 2021). We hypothesized that the pronounced seasonal change in labile biopolymers would considerably shift the relative abundances of biopolymer-degrading microbes between summer and fall. Furthermore, given the overlap of biochemical and microbial diversity datasets, we investigated whether individual DCCHO and DHAA components are linked to specific microbial taxa. Assessing relationships between the microbial community and the biopolymer pool over the seasonal cycle is important for understanding carbon cycling in the Arctic Ocean. The approach establishes a baseline of substrate regimes and their re-mineralization in the Fram Strait between summer and fall.

Experimental procedures

Sampling

Samples for biochemical and microbial analyses were collected in the upper 100 m of the water column using a rosette sampler equipped with 24 Niskin bottles. The rosette sampler was coupled to a CTD (SBE 911plus, Sea-bird, USA) equipped with two temperature probes, two conductivity probes, one Digiquartz pressure sensor, one WET Labs ECO-AFL/FL fluorometer, one WET Labs C-Star transmissometer and one altimeter. The sampling depths were chosen based on the output of the WET Labs ECO-AFL/FL fluorometer that was used to estimate phytoplankton biomass and identify the deep chlorophyll maximum (DCM). Specifically, four depths were of particular interest: surface (5 or 10 m), the DCM, below the DCM (BDCM), and 100 m. In summer, surface water was consistently sampled at 10 m, DCM at 20–43 m, and BDCM at 30–52 m. In fall, the surface water was sampled at 5 m, DCM at 20–34 m, and BDCM at 40–50 m. The DCM was distinct at all stations during summer and less clear during fall, but to be consistent, all mid-water column peaks of fluorescence were handled as the DCM during both seasons. The CTD data are archived in the PANGAEA World Data Center (von Appen *et al*., 2019; von Jackowski and Engel, 2019).

Particulate and dissolved organic matter

Samples for particulate organic carbon (POC) were collected by filtering 1 to 4 L of seawater onto 0.7 μm pore-sized pre-combusted GF/F filters (500°C, 4 h) and stored at −20°C. Back in the laboratory, the thawed filters were soaked in 0.1 M HCl to remove inorganic carbon, dried at 60°C for 12 h, and measured using a EURO EA CHNS-O Elemental Analyser (HEKAtech GmbH, Germany) (Sharp, 1974).

Data for corresponding samples of dissolved organic carbon (DOC), DCCHO and DHAA were incorporated from von Jackowski *et al*. (2020). In brief, DOC was analysed by the high-temperature catalytic oxidation method (TOC-VCSH, Shimadzu, Japan) (Sugimura and Suzuki, 1988; Qian and Mopper, 1996). DCCHO analysis was conducted by high-performance anion-exchange chromatography coupled with pulsed amperometric detection (HPAEC-PAD, ICS 3000, Dionex, USA) that classified 11 sugars: arabinose, fucose, galactose, galactosamine, galacturonic acid, glucose, glucosamine, glucuronic acid, rhamnose, and co-elute mannose and xylose (Engel and Händel, 2011). DHAA analysis was performed using ortho-phthaldialdehyde derivatization by high-performance liquid chromatography (Agilent, USA) that classified 13 monomers: alanine, arginine, aspartic acid, gamma-aminobutyric acid (GABA), glutamic acid, glycine, isoleucine, leucine, phenylalanine, serine, threonine, tyrosine and valine (Lindroth and Mopper, 1979; Dittmar *et al*., 2009).

Microbial production

Rates of primary production (PP) were measured *in situ* using the ^{14}C method modified after Engel *et al*. (2013). The seawater was incubated in duplicates with additional dark controls for a duration of 24 h. To also account for the changing diurnal cycle, the samples were incubated under constant light during summer, while the hours of light roughly matched the given day in fall. For example, incubation times decreased from 14 h (e.g. on 16.09.2018) at the beginning of the MSM77 expedition to 9.5 h (e.g. 04.10.2018) at the end of the MSM77 expedition.

Each incubation was fractionated and terminated in three subsamples: total PP (PP-TOC), particulate PP (PP-POC) and dissolved PP (PP-DOC). The PP-TOC fraction was taken directly from the incubation flask, the PP-POC fraction was filtered onto a 25 mm 0.4 μm-pore-sized Nucleopore track-etched polycarbonate filter (Whatman, GE Healthcare Life Sciences, UK), and the PP-DOC fraction was subsampled from the filtrate. To convert the activities into a rate, we converted total alkalinity into dissolved inorganic carbon using the package 'seacarb' (v.3.3.0). Data for the corresponding bacterial production (BP) based on the ^{3}H-microcentrifuge method (Smith and Azam, 1992) were incorporated from von Jackowski *et al*. (2020).

Cell abundance

Samples for cell abundance were fixed on board with glutardialdehyde at 2% final concentration and stored

frozen (−80°C) until analysis by flow cytometry (FACSCalibur, Becton Dickinson, USA). The flow cytometer was calibrated and standardized with TruCount beads (Becton Dickinson). Due to a detection limit of 50 μm, samples were filtered through a mesh before counting using the Cell Quest 3.3 software with a DL of 2000 events s^{-1}. Orange autofluorescence was used to detect the phycoerythrin of cyanobacteria (*Synechococcus*) and cryptophytes, whereas red fluorescence was used to detect and distinguish picoeukaryotes (<2 μm) from nanoeukaryotes (∼2–20 μm) (Read *et al*., 2014). Samples for heterotrophic cell analysis were filtered and stained with SybrGreenI (Invitrogen, USA), with data from the corresponding samples incorporated from von Jackowski *et al*. (2020).

Microbial community analysis

Seawater samples (1–4 L) were filtered through 0.22-μm Sterivex cartridges (Merck Millipore, USA) using a peristaltic pump within 1.5–2 h after retrieval of the CTD rosette and stored frozen (−80°C) until extraction. Filters were transferred from cartridges into kit-supplied tubes, and genomic DNA was isolated using a combined mechanical and chemical procedure using the PowerWater® DNA Isolation Kit (QIAGEN, Germany). Amplicon libraries were prepared according to the 16S Metagenomic Sequencing Library protocol (Illumina, USA) using universal 16S rRNA gene primers 515F and 926R that covered the V4–V5 hypervariable region (Parada *et al*., 2016). Sequences were acquired using a 2 × 300 bp paired-end run on a MiSeq platform (Illumina) at CeBiTec (Bielefeld, Germany). Sequence data have been deposited in the European Nucleotide Archive (ENA) at EMBL-EBI under accession number PRJEB43926, using the data brokerage service of the German Federation for Biological Data (GFBio; Diepenbroek *et al*., 2014) in compliance with MIxS standards (Yilmaz *et al*., 2011).

Sequence adaptors and primers were clipped using cutadapt, allowing a mismatch proportion error of 0.16 (Martin, 2011). Further processing was conducted in a server-based R installation (v3.6.0) to filter and merge reads into amplicon sequence variants (ASVs) using 'dada2' (v1.10.1; Callahan *et al*., 2016). ASVs were taxonomically classified using the SILVA SSU Reference dataset (release 132, 2018). ASVs matching chloroplast or mitochondrial sequences were removed, and only ASVs with >3 counts in more than 3% of samples were considered. We used 'phyloseq' (v1.30.0; McMurdie and Holmes, 2013) to manage sample data matrices. The 'iNEXT' package (v2.0.20; Hsieh *et al*., 2016) was used to calculate rarefaction curves, sample coverage and alpha-diversity indices.

Statistical analyses

Parameters that showed significant differences between the BDCM and 100 m were subsequently grouped into surface-to-BCDM ('surface', 'DCM' and 'BDCM') and 100 m. Detailed results of statistical analyses are documented in Table S2. Scripts are publically available at https://github.com/anabelvonjackowski.

Statistical analyses applied to the biogeochemical data included a Wilcoxon Rank Sum Test, analysis of variances (ANOVA) and a mixed model. If the interactive terms of the ANOVA were significant, they were fed into multiple contrast tests (Laird and Ware, 1982; Verbeke and Molenberghs, 2000) that included season ('summer', 'fall') and depth ('surface', 'DCM', 'BDCM' and '100 m') with the station as the random factor.

Statistical analyses applied to the amplicon data included ANOVAs, NMDS and $\log_2$fold-change ($\log_2$FC). PERMANOVAs with 999 permutations were based on season and depth using Bray–Curtis distances in the 'vegan' package (v2.5.7, 'adonis function'; Oksanen *et al*., 2019). NMDS was based on Bray–Curtis dissimilarities using the packages 'phyloseq' (v1.30.0 'ordinate' function; McMurdie and Holmes, 2013) and 'vegan' ('vegdist' function; Oksanen *et al*., 2019). Hierarchical cluster analysis of heatmaps was based on the 'complete' agglomeration method ('vegan' package 'hclust' function; Oksanen *et al*., 2019). $\log_2$FC calculated the enriched families and genera between seasons using an adjusted *p*-value of 0.05 using 'DESeq2' (v1.25.0; Love *et al*., 2014).

Microbial abundances and biopolymer concentrations were contextualized using Spearman rank correlation analysis using 'microbiomeSeq' package (v0.1, 'tax_env_cor' function; Ssekagiri and Ijaz, 2020). Additionally, variables were scaled ('vegan' package 'rda' function, scaled = TRUE) and selected ('vegan' package 'ordistep' function) during a forward selection by which the *p*-value was adjusted for multiple testing by Holm–Bonferroni.

Results and discussion

Study area

This study focused on eight stations within the Long-Term Ecological Research observatory HAUSGARTEN in the eastern Fram Strait (Soltwedel *et al*., 2016). Samples were collected during the expeditions PS114 with *RV Polarstern* from July 16th to July 23rd, 2018 (herein referred to as summer) and MSM77 with *RV Maria S. Merian* from September 16th to October 4th, 2018 (herein referred to as fall; Fig. 1A; Table S1). Four depths were of particular interest during this study: surface (5 or 10 m), the DCM, below the DCM (BDCM), and 100 m; in

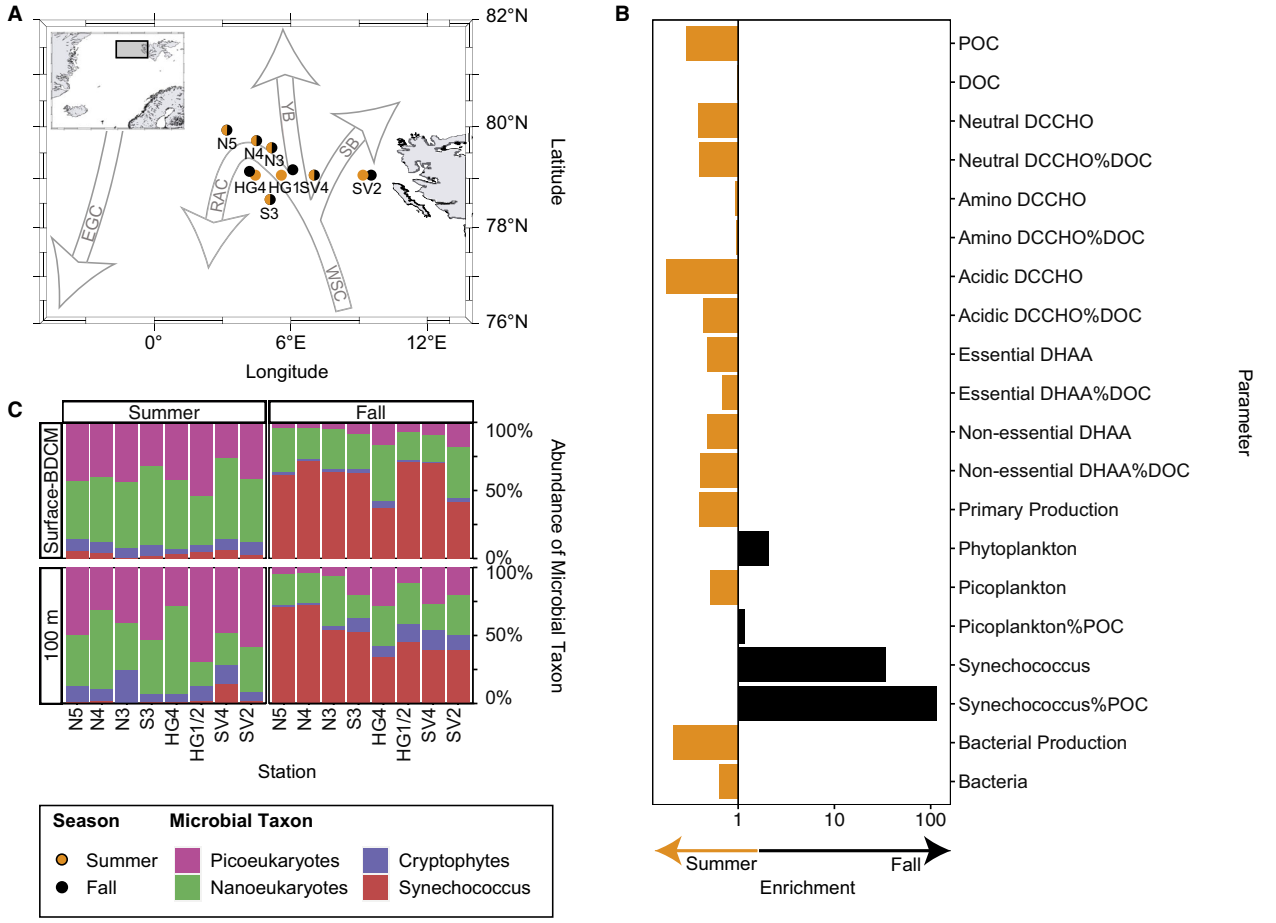

Fig. 1. Sampling sites, enrichment and relative abundance of phytoplankton in the upper 100 m during summer and fall.
A. Samples were taken onboard the RV Polarstern from July 16th to July 23rd, 2018 (orange) and the RV *Maria S. Merian* from September 16th to October 4th, 2018 (black). Arrows illustrate the main currents in the Fram Strait after Soltwedel *et al*. (2016).
B. Enrichments in the upper 100 m towards summer (left) and fall (right).
C. Relative abundance of autotrophs measured using flow cytometry in the surface (5 or 10 m) to BDCM (<50 m) and 100 m. Abbreviations: EGC, East Greenland Current; RAC, Return Atlantic Current; SB, Svalbard Branch; WSC, West Spitsbergen Current; YB, Yermark Branch; DOC, dissolved organic carbon; SLDOC, semi-labile DOC; POC, particulate organic carbon; PP; primary production; BP, heterotrophic bacterial production; BDCM, below deep chlorophyll maximum. Biogeochemical data (DOC, DCCHO, DHAA) and ecological data (BP, BA) from corresponding samples of von Jackowski *et al*. (2020).

summer, the DCM at 20–43 m and BDCM at 30–52 m; in fall, the DCM at 20–34 m and BDCM at 40–50 m.

In the upper 100 m, temperature increased slightly from 4.53 ± 1.45°C in summer (n = 32) to 5.35 ± 0.94°C in fall (n = 30, Fig. S1) (von Appen *et al*., 2019; von Jackowski and Engel, 2019). The salinity was 34.83 ± 0.48 PSU in summer (n = 32) and 34.90 ± 0.26 PSU in fall (n = 30) (von Appen *et al*., 2019; von Jackowski and Engel, 2019). These warm and saline conditions are characteristic of the Atlantic water masses in the West Spitsbergen Current (WSC; Aagaard *et al*., 1985) and likely displaced the ice edge north of 80°N during summer and fall. The intensity of the WSC is seasonally variable and influences the advection of carbon into the eastern Fram Strait, the major gateway between the Atlantic and Arctic Ocean (von Appen *et al*., 2016; Vernet *et al*., 2019).

Seasonal variability in POC and autotrophic microbes

POC decreased threefold in the upper 100 m from 18.07 ± 10.05 μmol L^{-1} in summer (n = 32) to 5.25 ± 3.78 μmol L^{-1} in fall (n = 32, Wilcoxon Rank Sum Test $p < 0.001$; Fig. 1B). The spatial variability of POC within the upper 100 m showed a significant twofold decrease below the deep chlorophyll maximum (BDCM; 30–52 m) and 100 m in summer, while no difference was observed during fall (ANOVA Season: Depth $F_{3,56} = 5.39$, $p < 0.01$; Multiple Contrast Test $p < 0.05$; Table S2). The seasonal change in POC concentrations was clearly related to phytoplankton dynamics, with a decline in chlorophyll-*a* (von Jackowski *et al*., 2020) and total biovolume (Lampe *et al*., 2021) from summer to fall in 2018.

PP decreased more than twofold in the dissolved organic carbon fraction (PP-DOC), with a significant threefold decrease in the particulate fraction (PP-POC) from summer to fall (Wilcoxon Rank Sum Test $p < 0.05$). PP-DOC declined from 1.74 ± 0.86 μmol C L^{-1} d^{-1} in summer ($n = 8$) to 0.62 ± 0.69 μmol C L^{-1} d^{-1} in fall ($n = 10$). PP-POC declined from 1.42 ± 1.68 μmol C L^{-1} d^{-1} in summer ($n = 8$) to 0.29 ± 0.39 μmol C L^{-1} d^{-1} in fall ($n = 10$). Simultaneously, cell abundances of cryptophytes and picoeukaryotes significantly decreased between summer and fall (Wilcoxon Rank Sum Test $p < 0.001$, Table S2). Cryptophyte abundances declined from 0.7 ± 0.4 cells L^{-1} in summer ($n = 32$) to 0.2 ± 0.2 cells L^{-1} in fall ($n = 32$), overall being significantly less abundant in the BDCM and 100 m (ANOVA Season:Depth $p < 0.05$, Multiple Contrast Test $p < 0.05$ and $p < 0.01$ respectively, Table S2). Similarly, picoeukaryote abundances declined from 4.5 ± 3.8 × 10^6 cells L^{-1} in summer ($n = 32$) to 2.3 ± 3.9 × 10^6 cells L^{-1} in fall ($n = 32$). Converting picoeukaryote abundances into carbon, by assuming a carbon biomass conversion factor of 530 fg C L^{-1} (Worden *et al*., 2004), showed that picoeukaryotes contributed 2.4 ± 2.0 μg C L^{-1} or 1.1% POC to the carbon pool in summer ($n = 32$) and 1.2 ± 2.1 μg C L^{-1} or 1.3% POC in fall ($n = 32$, Fig. 1B). Nanoeukaryotic abundance showed the least seasonal change and decreased from 5.1 ± 4.1 × 10^6 cells L^{-1} in summer ($n = 32$) to 4.9 ± 5.2 × 10^6 cells L^{-1} during fall ($n = 32$). It is likely that the PP-DOC fraction decreased as a result of declining cryptophyte, picoeukaryote and nanoeukaryote cell numbers. In particular, picoeukaryotes might be less influenced by temperature and salinity but instead driven by the seasonal light intensity and duration within the WSC (Paulsen *et al*., 2016). All in all, our data support the observed decline in relative biovolume from summer to fall in the eastern Fram Strait (Lampe *et al*., 2021).

Absolute and relative abundances of the cyanobacterium *Synechococcus* significantly increased from summer to fall, evident in both flow cytometry and 16S rRNA data (Wilcoxon Rank Sum Test $p < 0.001$, Table S2). *Synechococcus* abundances increased 34-fold from 0.4 ± 0.5 × 10^6 cells L^{-1} in summer ($n = 32$) to 14.6 ± 22.5 × 10^6 cells L^{-1} in fall ($n = 32$, Fig. 1B and C). Converting the *Synechococcus* abundances into carbon, by assuming a biomass conversion factor of 109.5 fg C L^{-1} (Kana and Glibert, 1987), showed that *Synechococcus* contributed 0.05 ± 0.05 μg C L^{-1} or 0.02% POC to the carbon pool in summer ($n = 32$) and subsequently increased 117-fold to 1.6 ± 2.5 μg C L^{-1} or 2.2% POC in fall ($n = 32$, Fig. 1B and C). According to our study and Paulsen *et al*. (2016), the seasonal pattern in *Synechococcus* abundances is as follows in the upper 100 m of the Fram Strait: 0.43 ± 0.45 × 10^6 cells L^{-1} in July (this study), 3.02 ± 3.79 × 10^6 cells L^{-1} in August

Table 1. Concentration, the contribution of DOC (%DOC) and relative composition (mol.%) of DCCHO in the water column.

		DOC	Neutral sugars			Acidic sugars			Amino sugars			
Season	Layer	nmol L^{-1}	nmol L^{-1}	DCCHO %DOC	mol.% DCCHO	nmol L^{-1}	DCCHO %DOC	mol.% DCCHO	μmol L^{-1}	DCCHO %DOC	mol.% DCCHO	*n*
Summer	Surface-100 m	72 063.75 ± 8885.33	749.05 ± 421.29	5.9 ± 3.4	92.9 ± 1.9	24.56 ± 18.98	1.5 ± 0.9	2.7 ± 1.5	31.44 ± 10.34	0.2 ± 0.1	4.4 ± 1.5	32
	Surface-BDCM	74 179.44 ± 8711.19	887.53 ± 397.69	6.8 ± 3.3	92.7 ± 1.7	31.03 ± 17.27	1.8 ± 0.7	3.2 ± 1.2	35.43 ± 7.96	0.3 ± 0.1	4.1 ± 1.3	24
	100 m	65 716.67 ± 6379.70	333.61 ± 57.68	3.0 ± 0.6	93.3 ± 2.5	5.16 ± 6.42	0.6 ± 0.7	1.3 ± 1.5	19.46 ± 6.84	0.2 ± 0.1	5.4 ± 1.6	8
Fall	Surface-100 m	71 646.34 ± 5682.32	287.55 ± 80.21	2.3 ± 0.7	89.5 ± 2.3	4.39 ± 5.32	0.7 ± 0.8	1.2 ± 1.4	29.22 ± 7.75	0.2 ± 0.1	9.3 ± 2.0	32
	Surface-BDCM	72 772.63 ± 5176.70	301.37 ± 83.84	2.4 ± 0.7	89.0 ± 1.9	5.08 ± 5.74	0.7 ± 0.9	1.3 ± 1.4	32.06 ± 6.66	0.3 ± 0.1	9.8 ± 1.8	24
	100 m	68 267.50 ± 6127.85	246.07 ± 52.68	2.1 ± 0.7	91.2 ± 2.6	2.30 ± 3.19	0.4 ± 0.6	0.8 ± 1.2	20.67 ± 3.02	0.2 ± 0.03	8.0 ± 2.2	8

DCCHO were differentiated into neutral sugars, acidic sugars and amino sugars. The DOC concentrations were incorporated from von Jackowski *et al*. (2020). '*n*' refers to the number of samples.

(Paulsen *et al*., 2016), 14.60 ± 22.54 × 10^6 cells L^{-1} in September/October (this study), and 0.48 ± 0.08 × 10^6 cells L^{-1} in November (Paulsen *et al*., 2016). This seasonal variability, as described here, could have far-reaching implications for the Arctic epipelagic carbon pool, given the low carbon-to-nitrogen ratios of Cyanobacteria (Finkel *et al*., 2016) and the biopolymer pool if *Synechococcus* employ an osmotrophic strategy (Yelton *et al*., 2016). Overall, there is a need for more continuous measurements to verify the seasonal variability and possible temperature-induced northward expansion of phytoplankton communities entering the Arctic Ocean through the Fram Strait (Orkney *et al*., 2020).

Quality of the biopolymer pool

To assess the carbohydrate content of the biopolymer pool, we differentiated DCCHO into neutral sugars, acidic sugars and amino sugars. Concentrations of neutral and acidic sugars significantly differed between summer and fall (Wilcoxon Rank Sum Test $p < 0.001$), particularly between the BDCM (30–52 m) and 100 m during summer (ANOVA Season:Depth $p < 0.01$; Multiple Contrast Test $p < 0.05$; Table S2). Neutral sugars accounted for the largest biopolymer proportion to the dissolved organic carbon pool (DCCHO%DOC) and molecular composition of the DCCHO pool (mol.%DCCHO, Table 1). The dominance of hydrolyzed glucose and mannose/xylose in summer (29 ± 11 and 31 ± 9 mol.% respectively) and fall (31 ± 8 and 37 ± 5 respectively) confirms that the North Atlantic transports relatively degraded DOC into the Arctic Ocean (Rich *et al*., 1997; Amon and Benner, 2003; Piontek *et al*., 2020). In addition, this study is among few others to report on the hydrolyzable acidic and amino sugar compositions in the North Atlantic and the Fram Strait (Engel *et al*., 2012; Grosse *et al*., 2021). Similar to neutral sugars, acidic sugars displayed a seasonal decrease in their concentration, DCCHO%DOC, and mol.%DCCHO (Table 1), which suggests a strong decline in freshly excreted DOC throughout the upper 100 m from summer to fall (Borchard and Engel, 2015). Amino sugars showed a twofold increase of mol.% DCCHO throughout the upper 100 m (Table 1), which might be explained by the presence of galacturonic acid and glucuronic acid in bacteria-derived DOC (Benner and Kaiser, 2003). As bacterial numbers decline towards fall, cell death or viral lysis release cellular-derived amino sugars into the surrounding water (Fig. 1B). The low decay coefficients of amino sugars make them resistant to decomposition and increase their residence time (Kawasaki and Benner, 2006), which results in the twofold increase of mol.%DCCHO until fall.

To assess the protein content of the biopolymer pool, we differentiated DHAA into essential amino acids (EAA)

Table 2. Concentration, the contribution of DOC (%DOC) and relative composition (mol.%) of DHAA in the water column.

Season	Layer	DOC	Essential amino acids			Non-essential amino acids			*n*
		nmol L^{-1}	nmol L^{-1}	DHAA%DOC	mol.%DHAA	nmol L^{-1}	DHAA%DOC	mol.%DHAA	
Summer	Surface-100 m	72 063.75 ± 8885.33	189.94 ± 88.86	1.0 ± 0.5	47.9 ± 3.9	219.64 ± 127.94	1.2 ± 0.7	52.1 ± 3.9	32
	Surface-BDCM	74 179.44 ± 8711.19	219.81 ± 81.76	1.2 ± 0.5	46.4 ± 2.9	261.89 ± 119.59	1.4 ± 0.7	53.6 ± 2.9	24
	100 m	65 716.67 ± 6379.70	100.31 ± 27.73	0.6 ± 0.2	52.4 ± 3.3	92.88 ± 31.79	0.5 ± 0.2	47.6 ± 3.3	8
Fall	Surface-100 m	71 646.34 ± 5682.32	90.59 ± 26.90	0.4 ± 0.2	50.8 ± 2.1	89.24 ± 33.64	0.5 ± 0.2	49.2 ± 2.1	31
	Surface-BDCM	72 772.63 ± 5176.70	95.29 ± 27.86	0.4 ± 0.2	50.3 ± 2.0	95.45 ± 35.37	0.5 ± 0.2	49.7 ± 2.0	23
	100 m	68 267.50 ± 6127.85	77.07 ± 19.51	0.4 ± 0.1	52.1 ± 1.9	71.40 ± 20.65	0.4 ± 0.1	47.9 ± 1.9	8

DHAA were differentiated into EAA and NEAA. The DOC concentrations were incorporated from von Jackowski *et al*. (2020). '*n*' refers to the number of samples.

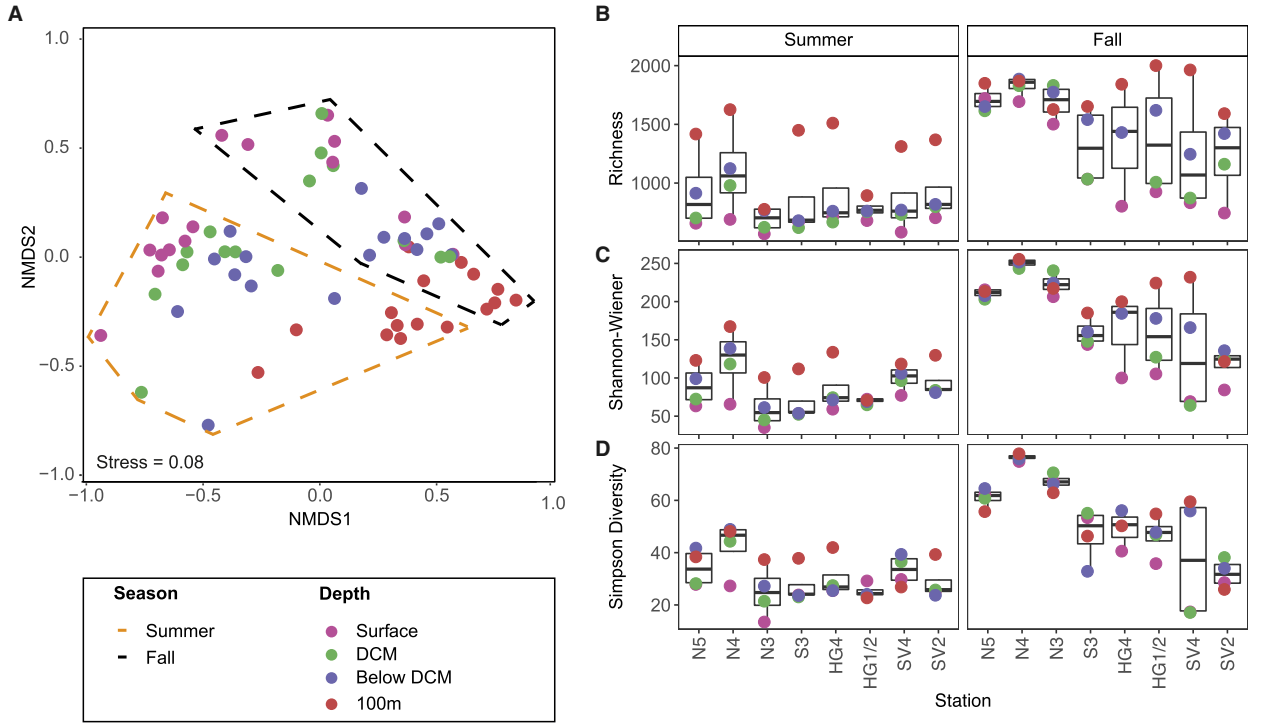

Fig. 2. Ordination and diversity of microbial community during summer and fall.
A. NMDS based on Bray–Curtis dissimilarities of ASV counts, i.e. highest taxonomic resolution, with depth (surface, 5–10 m; DCM, 20–40 m; BDCM, ∼50 m; 100 m) and station illustrated by colours and shapes respectively (stress: 0.08).
B. Box plot indicating species richness.
C. Box plot indicating Shannon–Wiener diversity index (SDI).
D. Box plot indicating the inverse Simpson diversity index. DCM, deep chlorophyll maximum; BDCM, below deep chlorophyll maximum.

and non-essential amino acids (NEAA). Phytoplankton can synthesize both EAAs and NEAA depending on their nutrient limitation, while higher trophic levels rely on the acquisition of EAA through their diet and acquisition or *de novo* synthesis of NEAA (Arts *et al*., 2009; Grosse *et al*., 2019; Larsen *et al*., 2022). Concentrations of EAA and NEAA decreased significantly between summer and fall (Table 2; Wilcoxon Rank Sum Test $p < 0.001$). The significant reduction in the amino acid reservoir is indicative of the utilization of nitrogen-rich compounds from summer to fall. Furthermore, EAA and NEAA concentrations during fall are representative of post-bloom conditions; i.e. EAA: 89.7 nmol L^{-1}, 0.5 DHAA%DOC, and 50.4 mol.%DHAA; NEAA: 90.6 nmol L^{-1}, 0.5 DHAA% DOC, and 49.6 mol.%DHAA in upper 100 m of the eastern Fram Strait in 2017 (Grosse *et al*., 2021) (Table 2).

Microbial community composition in context of biopolymer pool

Amplicon sequencing of the 16S rRNA V4–V5 hypervariable region resulted in 4 872 711 sequences assigned to 2960 ASVs. Alpha-diversity analyses covered more than 80% of the sequence richness (Fig. S2). Microbial species richness and evenness (Shannon–Wiener index, inverse Simpson index) significantly decreased between summer and fall (Fig. 2, Wilcoxon Rank Sum Test $p < 0.001$, ANOVA $p < 0.01$, Table S2). Additionally, the non-metric multidimensional scaling (NMDS) illustrated the significant differences by season and depth (Fig. 2, ANOSIM $p < 0.05$, Table S2).

Around 81% ASVs were shared between summer and fall, illustrating a considerable number of taxa that do not respond to the changing biopolymer pool and other seasonal changes (Wietz *et al*., 2021). Common taxa were defined as ASVs with >3 counts, >3% sequence abundance, and occurred in all the samples. Common taxa significantly differed between the surface-to-BCDM and 100 m (ANOSIM $p < 0.01$, Table S2). Within the surface-to-BCDM, some common taxa like Planktomarina and SAR11 clades significantly correlated with hydrolyzed acidic sugars (+, summer), serine (+, fall) and glycine (−) during both seasons (Figs 3 and 4). At 100 m, common taxa exhibited significant correlations with isoleucine (+) and glucose (−) during both seasons (Fig. 4C and D).

The predominance of labile biopolymers like fucose, rhamnose and threonine coincided with lower microbial diversity, illustrated by 3% of ASVs that were exclusively detected during summer (Fig. 2, Fig. S3). In particular, the *SAR92* clade was significantly enriched in the surface-to-

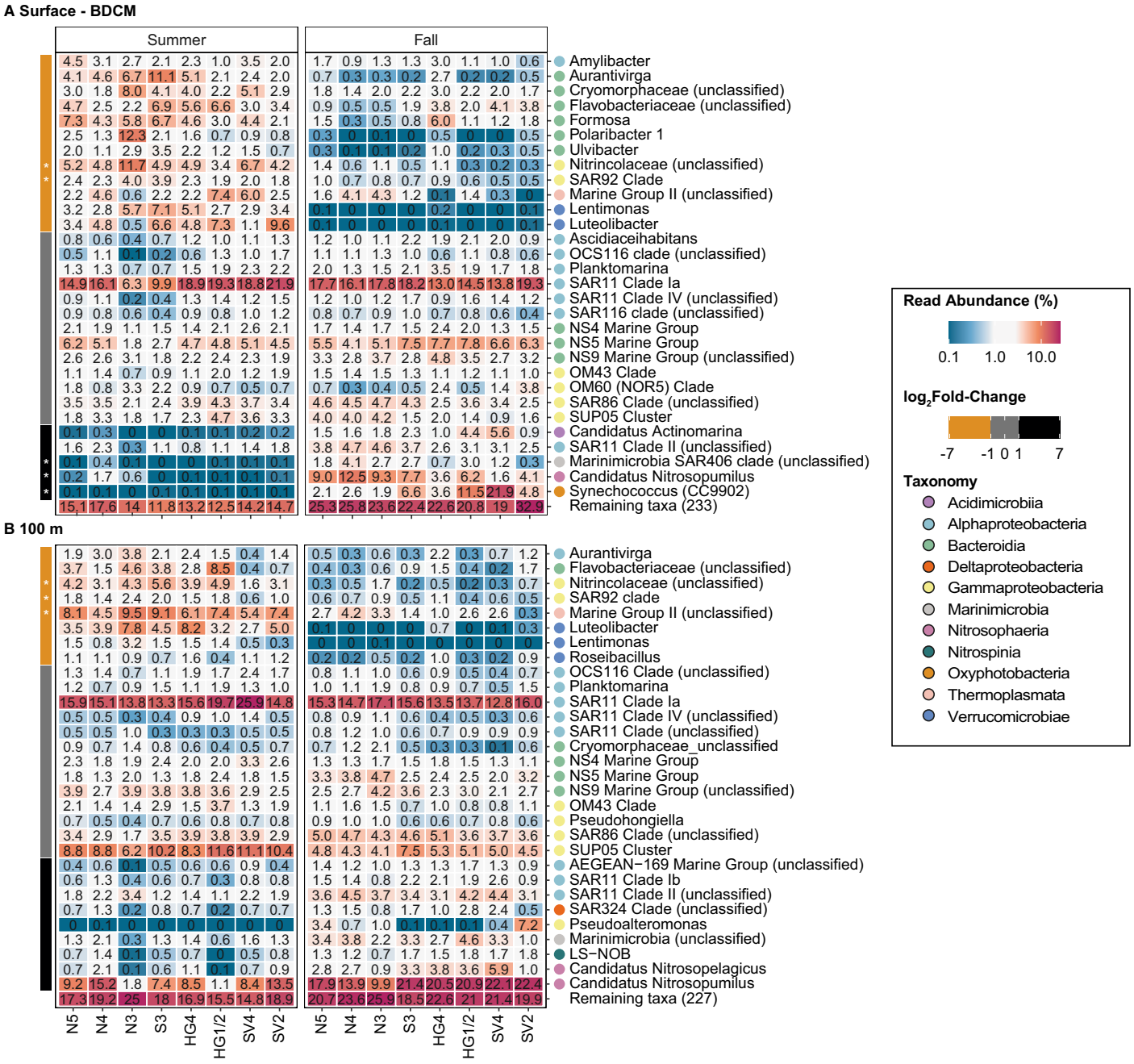

Fig. 3. Relative abundance with enrichments in the upper 100 m during summer and fall.
A. Relative abundance of top 30 genera in the surface – BDCM (5–50 m) were averaged due to the lack of significant differences between these depths (see text).
B. Relative abundance of top 30 genera in 100 m. The enrichments (coloured bars) between the seasons were calculated using $\log_2$Fold-Change (orange = summer, black = fall, grey = no seasonal enrichment) with significant differences marked by an asterisk ($p_{adj} < 0.05$) – Abbreviation: BDCM, below deep chlorophyll maximum.

BDCM in summer (Fig. 3A, $\log_2FC = 3.7$ $q < 0.01$), which might be linked to the abundance of *Phaeocystis* colonies in the Fram Strait (Lampe *et al*., 2021; Wietz *et al*., 2021). Additionally, we observed high relative abundances of the *Flavobacteriaceae* genera *Aurantivirga*, *Formosa*, *Polaribacter* and *Ulvibacter* (Fig. 3A), with significant positive correlations to labile compounds like fucose and threonine (Fig. 4A). Fucose significantly constrained the ordination space of the redundancy analysis (RDA), suggesting the importance of fucose containing polymers for polysaccharide-degrading taxa (forward selection, $F = 3.6$, $q < 0.05$; Fig. 5) (Cottrell and Kirchman, 2000; Buchan

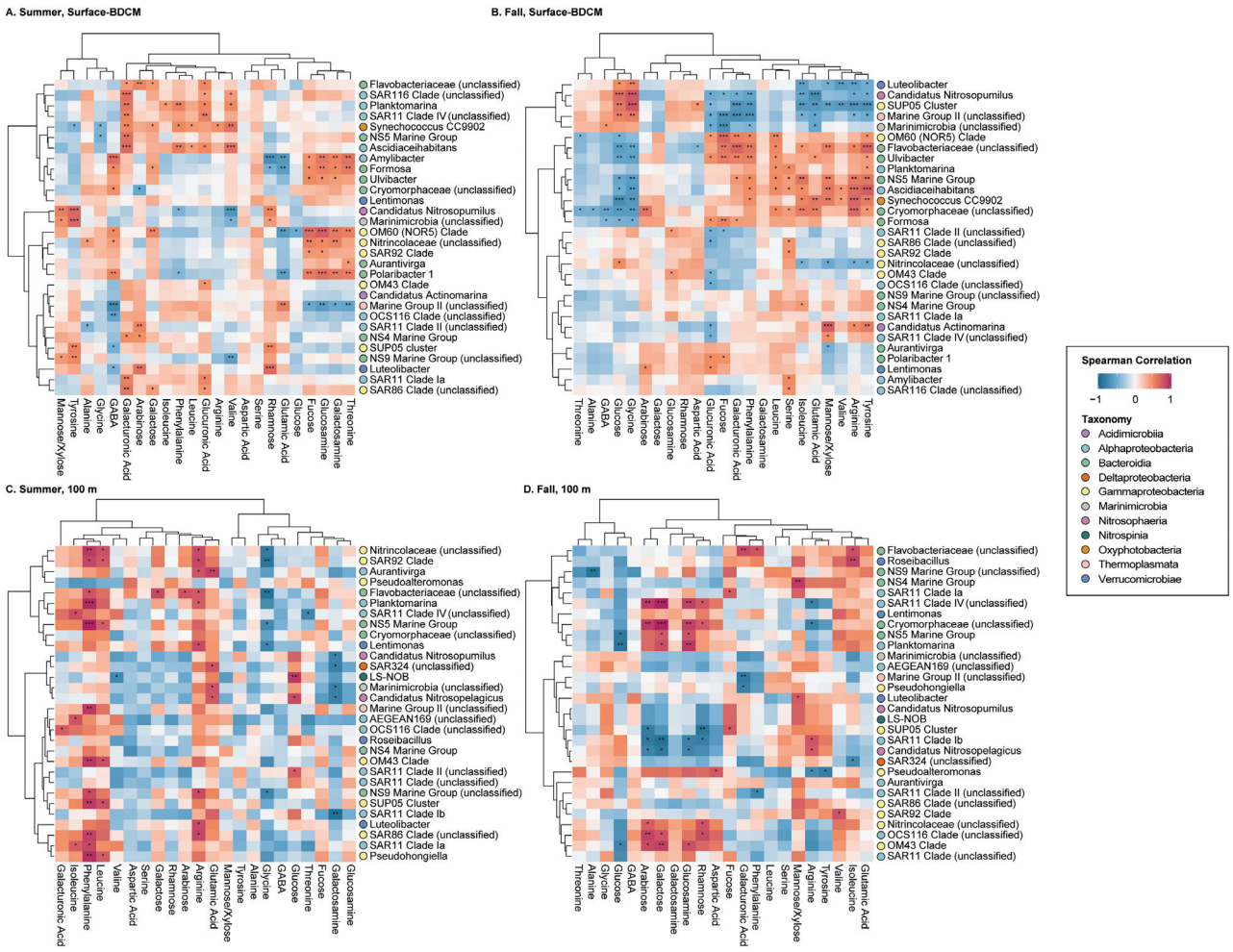

Fig. 4. Spearman rank correlation matrix of genera and biopolymers in the upper 100 m during summer and fall.
A. Correlations of top 30 genera in surface – BDCM (10–50 m) due to lack of significant differences between these depths during summer.
B. Correlations of top 30 genera in surface – BDCM (5–50 m) due to lack of significant differences between these depths during fall.
C. Correlations of top 30 genera in 100 m during summer.
D. Correlations of top 30 genera in 100 m during fall. The clusters were performed using 'complete' clusters analysis and the spearman correlation (blue to red) was performed and associated with adjusted *p*-values for multiple testing. Abbreviations: BDCM, below deep chlorophyll maximum. Corresponding biopolymer data were retrieved from von Jackowski *et al*. (2020). Significance codes are shown by asterisks: '***' < 0.001,'**' < 0.01,'*' < 0.05 and >0.05.

et al., 2014; Reintjes *et al*., 2019). Furthermore, *Formosa* and *Polaribacter* show significant positive correlations to GABA (Fig. 4A). Hence these taxa might be actively growing in the surface-to-BDCM, since GABA can serve as an indicator for microbial activity and might portray amino acid turnover more accurately than ^{3}H-leucine-derived BP, which can substantially underestimate bacterial growth (Popendorf *et al*., 2020). At 100 m, we observed a significant increase of *Candidatus* Nitrosopumilus, *LS-NOB* and unclassified Marine Group II archaea (all $\log_2$FC, $q < 0.01$, Figs 3 and 4; Table S2). The shift towards taxa that are typically observed in low light waters suggests that the microbial community is already beginning to target low-molecular-weight DOM.

16% of ASVs were exclusively detected during fall (Fig. 2, Fig. S3). The significant enrichment of *Synechococcus* in the surface-to-BDCM corresponds to flow cytometry-derived cell counts ($\log_2$FC $q < 0.05$, Figs 1 and 2; Table S2). Additionally, the relative abundance of *Candidatus* Nitrosopumilus and Marinimicrobia (SAR406 clade) significantly increased from summer to fall ($\log_2$FC $q < 0.05$, Fig. 3; Table S2), which negatively correlated with more labile compounds (i.e. fucose, isoleucine, phenylalanine) but positively correlated with more refractory compounds (i.e. alanine, aspartic acid and glycine; Fig. 4). *Candidatus* Nitrosopelagicus and *Candidatus* Nitrosopumilus showed the highest abundances in 100 m during fall ($\log_2$FC $q < 0.05$, Fig. 3; Table S2). Generally, more

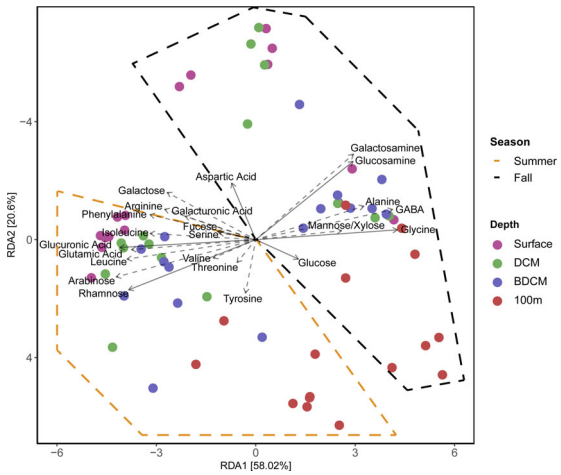

Fig. 5. RDA based on Hellinger transformed samples. The continuous arrows correspond to the significant forward-selected variables, while the dashed arrows correspond to the remaining parameters included in this study. The boxes were manually added to the figure to add the seasonal separation. Abbreviations: GABA, gamma-aminobutyric acid. Data for dissolved parameters and gel particle data from corresponding samples by von Jackowski *et al*. (2020).

refractory compounds were the biogeochemical divers for the microbial community in fall (Fig. 5). Glycine, for example, has been shown to have low microbial degradation rates (Veuger *et al*., 2012), which suggests that more refractory biopolymers either accumulate or are synthesized during fall. Particularly, *Candidatus* Nitrosopumilus have been linked to continuously releasing glycine but also alanine, valine, leucine, isoleucine, phenylalanine during ammonia oxidation (Bayer *et al*., 2019). Moreover, the presence of ammonia-oxidizing archaea and nitrite-oxidizing bacteria, like LS-NOB, indicate beginning nitrate replenishment at the start of the polar night (Fig. 4B).

Conclusion

Our assessment of microbial communities in the context of the organic matter pool identified autotrophic and heterotrophic seasonality in the Fram Strait, and their association with different biopolymers. Seasonal variability of autotrophic microbes was closely related to a decline in POC, production rates and cell abundances. The most notable seasonal shift was observed in *Synechococcus* that can use their osmotrophy strategy to compete for biopolymers with heterotrophic microbes (Yelton *et al*., 2016). Among the heterotrophic community, the lower alpha-diversity suggests that specialized groups target labile biopolymers in summer, while a higher alpha-diversity suggests that taxa including ammonia and nitrite oxidizers scavenge for more refractory substrates in fall. Our study highlights seasonally driven associations between biopolymers and microbial community, yet studying these associations under varying environmental conditions (e.g. sea ice versus ice free) and higher resolution approaches (e.g. transcriptomics), could truly explain the microbial substrate regimes in the Arctic Ocean.

Acknowledgements

We thank the RV *Polarstern* and RV *Maria S. Merian* crews for their support during the sample acquisition. Special thanks to Jana Bäger, Jakob Barz, Nadine Knüppel, Sandra Murawski, Swantje Rogge, Tania Klüver, Jon Roa and Sandra Golde for sampling onboard and laboratory analyses. We also give thanks to Julia Grosse, who sampled for primary production onboard RV *Polarstern*. Sampling for bacterial sequence analyses was carried out in the framework of the HGF infrastructure program FRAM (Frontiers in Arctic Marine Monitoring). We are very grateful for the comments from the reviewers that greatly improved the manuscript. The work was funded by the Helmholtz Association and by the MicroARC project (03F0802A) within the Changing Arctic Ocean program, jointly funded by the UKRI Natural Environment Research Council (NERC) and the German Federal Ministry of Education and Research (BMBF). Open Access funding was enabled and organized by project MicroARC (03F0802A). RV *Polarstern* was funded under grant AWI_PS114_01. Open Access funding enabled and organized by Projekt DEAL.

Authors' Contributions

AvJ and AE conceived the study. AvJ, MW and CB coordinated the sampling. MW processed the sequence data. AvJ analysed and interpreted the data and primarily wrote the manuscript with contributions from all co-authors.

Data Availability

Environmental data are archived in the PANGAEA World Data Center under the accession numbers 942618 and 942624. Amplicon data are archived in the ENA at EMBL-EBI under accession number PRJEB43926.

References

Aagaard, K., Swift, J.H., and Carmack, E.C. (1985) Thermohaline circulation in the Arctic Mediterranean Seas. *J Geophys Res* **90**: 4833–4846.

Amon, R.M.W., and Benner, R. (2003) Combined neutral sugars as indicators of the diagenetic state of dissolved organic matter in the Arctic Ocean. *Deep Res Part I Oceanogr Res Pap* **50**: 151–169.

Arts, M.T., Brett, M.T., and Kainz, M.J. (2009) *Lipids in Aquatic Ecosystems*. Dordrecht, The Netherlands: Springer.

Bayer, B., Hansman, R.L., Bittner, M.J., Noriega-Ortega, B. E., Niggemann, J., Dittmar, T., and Herndl, G.J. (2019)

Ammonia-oxidizing archaea release a suite of organic compounds potentially fueling prokaryotic heterotrophy in the ocean. *Environ Microbiol* **21**: 4062–4075.

Benner, R., and Kaiser, K. (2003) Abundance of amino sugars and peptidoglycan in marine particulate and dissolved organic matter. *Limnol Oceanogr* **48**: 118–128.

Benner, R., Pakulski, J.D., McCarthy, M., Hedges, J.I., and Hatcher, P.G. (1992) Bulk chemical characteristics of dissolved organic matter in the ocean. *Science* **255**: 1561–1564.

Biersmith, A., and Benner, R. (1998) Carbohydrates in phytoplankton and freshly produced dissolved organic matter. *Mar Chem* **63**: 131–144.

Boetius, A., Anesio, A.M., Deming, J.W., Mikucki, J.A., and Rapp, J.Z. (2015) Microbial ecology of the cryosphere: sea ice and glacial habitats. *Nat Rev Microbiol* **13**: 677–690.

Borchard, C., and Engel, A. (2015) Size-fractionated dissolved primary production and carbohydrate composition of the coccolithophore Emiliania huxleyi. *Biogeosciences* **12**: 1271–1284.

Buchan, A., LeCleir, G.R., Gulvik, C.A., and González, J.M. (2014) Master recyclers: features and functions of bacteria associated with phytoplankton blooms. *Nat Rev Microbiol* **12**: 686–698.

Callahan, B.J., McMurdie, P.J., Rosen, M.J., Han, A.W., Johnson, A.J.A., and Holmes, S.P. (2016) DADA2: high-resolution sample inference from Illumina amplicon data. *Nat Methods* **13**: 581–587.

Cardozo Mino, M.G., Fadeev, E., Salman-Carvalho, V., and Boetius, A. (2021) Spatial dynamics in Arctic bacterioplankton community densities are strongly linked to distinct physical and biological processes (Fram Strait, 79°N). *Front Microbiol* **12**: 1–14.

Cottrell, M.T., and Kirchman, D.L. (2000) Natural assemblages of marine proteobacteria and members of the Cytophaga-Flavobacter cluster consuming low- and high-molecular-weight dissolved organic matter. *Appl Environ Microbiol* **66**: 1692–1697.

Diepenbroek, M., Glöckner, F.O.F.O., Grobe, P., Güntsch, A., Huber, R., König-Ries, B., *et al*. (2014) Towards an integrated biodiversity and ecological research data management and archiving platform: the German federation for the curation of biological data (GFBio). In *Informatik 2014*. Bonn: Gesellschaft für Informatik e.V., pp. 1711–1721.

Dittmar, T., Cherrier, J., and Ludwichowski, K.-U. (2009) The analysis of amino acids in seawater. In *Practical Guidelines for the Analysis of Seawater*, Wurl, O. (ed). FL, USA: CRC Press, Taylor & Francis Group, pp. 67–77.

Engel, A., Borchard, C., Piontek, J., Schulz, K.G., Riebesell, U., and Bellerby, R. (2013) CO_2 increases 14C primary production in an Arctic plankton community. *Biogeosciences* **10**: 1291–1308.

Engel, A., and Händel, N. (2011) A novel protocol for determining the concentration and composition of sugars in particulate and in high molecular weight dissolved organic matter (HMW-DOM) in seawater. *Mar Chem* **127**: 180–191.

Engel, A., Handel, N., Wohlers, J., Lunau, M., Grossart, H.-P., Sommer, U., and Riebesell, U. (2011) Effects of sea surface warming on the production and composition of dissolved organic matter during phytoplankton blooms: results from a mesocosm study. *J Plankton Res* **33**: 357–372.

Engel, A., Harlay, J., Piontek, J., and Chou, L. (2012) Contribution of combined carbohydrates to dissolved and particulate organic carbon after the spring bloom in the northern Bay of Biscay (North-Eastern Atlantic Ocean). *Cont Shelf Res* **45**: 42–53.

Fadeev, E., Salter, I., Schourup-Kristensen, V., Nöthig, E.-M., Metfies, K., Engel, A., *et al*. (2018) Microbial communities in the east and west Fram Strait during sea ice melting season. *Front Mar Sci* **5**: 1–21.

Finkel, Z.V., Follows, M.J., Liefer, J.D., Brown, C.M., Benner, I., and Irwin, A.J. (2016) Phylogenetic diversity in the macromolecular composition of microalgae. *PLoS One* **11**: 1–16.

Grosse, J., Brussaard, C.P.D., and Boschker, H.T.S. (2019) Nutrient limitation driven dynamics of amino acids and fatty acids in coastal phytoplankton. *Limnol Oceanogr* **64**: 302–316.

Grosse, J., Nöthig, E.-M., Torres-Valdés, S., and Engel, A. (2021) Summertime amino acid and carbohydrate patterns in particulate and dissolved organic carbon across Fram Strait. *Front Mar Sci* **8**: 1–15.

Hansell, D., Carlson, C., Repeta, D., and Schlitzer, R. (2009) Dissolved organic matter in the ocean: a controversy stimulates new insights. *Oceanography* **22**: 202–211.

Hedges, J.I., Baldock, J.A., Gélinas, Y., Lee, C., Peterson, M.L., and Wakeham, S.G. (2002) The biochemical and elemental compositions of marine plankton: A NMR perspective. *Mar Chem* **78**: 47–63.

Hsieh, T.C., Ma, K.H., and Chao, A. (2016) iNEXT: an R package for rarefaction and extrapolation of species diversity (Hill numbers). *Methods Ecol Evol* **7**: 1451–1456.

Kana, T.M., and Glibert, P.M. (1987) Effect of irradiances up to 2000 $\mu E\ m^{-2}\ s^{-1}$ on marine Synechococcus WH7803—I. Growth, pigmentation, and cell composition. *Deep Sea Res Part A Oceanogr Res Pap* **94**: 479–495.

Kawasaki, N., and Benner, R. (2006) Bacterial release of dissolved organic matter during cell growth and decline: Molecular origin and composition. *Limnol Oceanogr* **51**: 2170–2180.

Kirchman, D.L., Cottrell, M.T., and Lovejoy, C. (2010) The structure of bacterial communities in the western Arctic Ocean as revealed by pyrosequencing of 16S rRNA genes. *Environ Microbiol* **12**: 1132–1143.

Laird, N.M., and Ware, J.H. (1982) Random-effects models for longitudinal data. *Biometrics* **38**: 963.

Lampe, V., Nöthig, E.-M., and Schartau, M. (2021) Spatiotemporal variations in community size structure of Arctic protist plankton in the Fram Strait. *Front Mar Sci* **7**: 1–18.

Larsen, T., Wang, Y.V., and Wan, A.H.L. (2022) Tracing the trophic fate of aquafeed macronutrients with carbon isotope ratios of amino acids. *Front Mar Sci* **9**: 1–14.

Lindroth, P., and Mopper, K. (1979) High performance liquid chromatographic determination of subpicomole amounts of amino acids by precolumn fluorescence derivatization with o-phthaldialdehyde. *Anal Chem* **51**: 1667–1674.

Love, M.I., Huber, W., and Anders, S. (2014) Moderated estimation of fold change and dispersion for RNA-seq data with DESeq2. *Genome Biol* **15**: 1–21.

Martin, M. (2011) Cutadapt removes adapter sequences from high-throughput sequencing reads. *EMBnetJ* **17**: 10–12.

McMurdie, P.J., and Holmes, S. (2013) phyloseq: an R package for reproducible interactive analysis and graphics of microbiome census data. *PLoS One* **8**: 1–11.

Oksanen, J., Blanchet, F.G., Friendly, M., Kindt, R., Legendre, P., Mcglinn, D., *et al*. (2019) Package "vegan" Community Ecology Package Version 2.5-6.

Orkney, A., Platt, T., Narayanaswamy, B.E., Kostakis, I., and Bouman, H.A. (2020) Bio-optical evidence for increasing Phaeocystis dominance in the Barents Sea. *Philos Trans A Math Phys Eng Sci* **378**: 1–16.

Parada, A.E., Needham, D.M., and Fuhrman, J.A. (2016) Every base matters: assessing small subunit rRNA primers for marine microbiomes with mock communities, time series and global field samples. *Environ Microbiol* **18**: 1403–1414.

Paulsen, M.L., Doré, H., Garczarek, L., Seuthe, L., Müller, O., Sandaa, R.-A., *et al*. (2016) Synechococcus in the Atlantic gateway to the Arctic Ocean. *Front Mar Sci* **3**: 1–14.

Piontek, J., Galgani, L., Nöthig, E.-M., Peeken, I., and Engel, A. (2020) Organic matter composition and heterotrophic bacterial activity at declining summer sea ice in the central Arctic Ocean. *Limnol Oceanogr* **66**: 1–20.

Piontek, J., Sperling, M., Nöthig, E.-M., and Engel, A. (2014) Regulation of bacterioplankton activity in Fram Strait (Arctic Ocean) during early summer: The role of organic matter supply and temperature. *J Mar Syst* **132**: 83–94.

Popendorf, K.J., Koblížek, M., and Van Mooy, B.A.S. (2020) Phospholipid turnover rates suggest that bacterial community growth rates in the open ocean are systematically underestimated. *Limnol Oceanogr* **65**: 1876–1890.

Qian, J., and Mopper, K. (1996) Automated high-performance, high-temperature combustion total organic carbon analyzer. *Anal Chem* **68**: 3090–3097.

Randelhoff, A., Reigstad, M., Chierici, M., Sundfjord, A., Ivanov, V., Cape, M., *et al*. (2018) Seasonality of the physical and biogeochemical hydrography in the inflow to the Arctic Ocean through Fram Strait. *Front Mar Sci* **5**: 1–16.

Read, D.S., Bowes, M.J., Newbold, L.K., and Whiteley, A.S. (2014) Weekly flow cytometric analysis of riverine phytoplankton to determine seasonal bloom dynamics. *Environ Sci Process Impacts* **16**: 594–603.

Reintjes, G., Arnosti, C., Fuchs, B., and Amann, R. (2019) Selfish, sharing and scavenging bacteria in the Atlantic Ocean: a biogeographical study of bacterial substrate utilisation. *ISME J* **13**: 1119–1132.

Rich, J., Gosselin, M., Sherr, E., Sherr, B., and Kirchman, D. L. (1997) High bacterial production, uptake and concentrations of dissolved organic matter in the Central Arctic Ocean. *Deep Sea Res Part II Top Stud Oceanogr* **44**: 1645–1663.

Sharp, J.H. (1974) Improved analysis for "particulate" organic carbon and nitrogen from seawater. *Limnol Oceanogr* **19**: 984–989.

Smith, D.C., and Azam, F. (1992) A simple, economical method for measuring bacterial protein synthesis rates in seawater using 3H-leucine. *Mar Microb Food Webs* **6**: 107–114.

Soltwedel, T., Bauerfeind, E., Bergmann, M., Bracher, A., Budaeva, N., Busch, K., *et al*. (2016) Natural variability or anthropogenically-induced variation? Insights from 15 years of multidisciplinary observations at the arctic marine LTER site HAUSGARTEN. *Ecol Indic* **65**: 89–102.

Ssekagiri, A., and Ijaz, U.Z. (2020) microbiomeSeq: microbial community analysis in an environmental context.

Sugimura, Y., and Suzuki, Y. (1988) A high-temperature catalytic oxidation method for the determination of non-volatile dissolved organic carbon in seawater by direct injection of a liquid sample. *Mar Chem* **24**: 105–131.

Teeling, H., Fuchs, B.M., Becher, D., Klockow, C., Gardebrecht, A., Bennke, C.M., *et al*. (2012) Substrate-controlled succession of marine bacterioplankton populations induced by a phytoplankton bloom. *Science* **336**: 608–611.

Verbeke, G., and Molenberghs, G. (2000) *Linear Mixed Models For Longitudinal Data*. NY, USA: Springer.

Vernet, M., Ellingsen, I.H., Seuthe, L., Slagstad, D., Cape, M.R., and Matrai, P.A. (2019) Influence of phytoplankton advection on the productivity along the Atlantic water inflow to the Arctic Ocean. *Front Mar Sci* **6**: 1–18.

Veuger, B., van Oevelen, D., and Middelburg, J.J. (2012) Fate of microbial nitrogen, carbon, hydrolysable amino acids, monosaccharides, and fatty acids in sediment. *Geochim Cosmochim Acta* **83**: 217–233.

von Appen, W.J., Schaffer, J., Rohardt, G., and Wisotzki, A. (2019) Physical oceanography measured on water bottle samples during POLARSTERN cruise PS114 Accession: 898695.

von Appen, W.J., Schauer, U., Hattermann, T., and Beszczynska-Möller, A. (2016) Seasonal cycle of mesoscale instability of the West Spitsbergen Current. *J Phys Oceanogr* **46**: 1231–1254.

von Jackowski, A., and Engel, A. (2019) Physical oceanography measured on water bottle samples during Maria S. Merian cruise MSM77 Accession: 907467.

von Jackowski, A., Grosse, J., Nöthig, E.-M., and Engel, A. (2020) Dynamics of organic matter and bacterial activity in the Fram Strait during summer and autumn. *Philos Trans R Soc A Math Phys Eng Sci* **378**: 1–16.

Wietz, M., Bienhold, C., Metfies, K., Torres-Valdés, S., von Appen, W.J., Salter, I., and Boetius, A. (2021) The polar night shift: seasonal dynamics and drivers of Arctic Ocean microbiomes revealed by autonomous sampling. *ISME Commun* **1**: 1–12.

Wilson, B., Müller, O., Nordmann, E.-L., Seuthe, L., Bratbak, G., and Øvreås, L. (2017) Changes in marine prokaryote composition with season and depth over an Arctic polar year. *Front Mar Sci* **4**: 1–17.

Worden, A.Z., Nolan, J.K., and Palenik, B. (2004) Assessing the dynamics and ecology of marine picophytoplankton: the importance of the eukaryotic component. *Limnol Oceanogr* **49**: 168–179.

Yelton, A.P., Acinas, S.G., Sunagawa, S., Bork, P., Pedrós-Alió, C., and Chisholm, S.W. (2016) Global genetic capacity for mixotrophy in marine picocyanobacteria. *ISME J* **10**: 2946–2957.

Yilmaz, P., Kottmann, R., Field, D., Knight, R., Cole, J.R., Amaral-Zettler, L., *et al*. (2011) Minimum information about a marker gene sequence (MIMARKS) and minimum

information about any (x) sequence (MIxS) specifications. *Nat Biotechnol* **29**: 415–420.

Supporting Information

Additional Supporting Information may be found in the online version of this article at the publisher's web-site:

Fig. S1. Environmental conditions during summer and fall in the Fram Strait. A. The temperature by latitude and longitude during summer. B. The temperature by latitude and longitude during fall. C. The fluorescence, temperature, and salinity were measured using the CTD at 'HG4' during summer and fall. The fluorescence was measured using a WET Labs ECO-AFL/FL fluorometer, the temperature was measured using a SEA-BIRD temperature probe, and salinity was measured using a SEA-BIRD conductivity probe. The horizontal lines indicate the sampling depths of the surface, DCM, BDCM, and 100 m. The DCM was distinct at all stations during summer and less clear during fall, but to be consistent. Abbreviation: DCM, deep chlorophyll maximum; BDCM, below deep chlorophyll maximum.

Fig. S2. Rarefaction curves of samples between summer and fall in the Fram Strait. The colours represent the season.

Fig. S3. Venn diagrams of shared ASVs between the microbial community. A. Summer compared to fall. B–H. All the depths sampled in the upper 100 m.

Table S1. List of stations and parameters sampled during RV Polarstern expedition PS114 and RV Maria S. Merian expedition MSM77.

Table S2. Summary of statistical tests with significant p-values in bold. Abbreviation: ANOVA, Analysis of Variance; DOF, Degree of Freedom; Richness, Observed Richness.